Superhydrophobic surface fabricated by spraying hydrophobic R974 nanoparticles and the drag reduction in water

Chujiang Cai [a,b,*], Nannan Sang [a], Sicong Teng [c], Zhigang Shen [a], Jiang Guo [b], Xiaohu Zhao [c], Zhanhu Guo [b,**]

[a] Beijing Key Laboratory for Powder Technology Research and Development, Beihang University, Beijing 100191, PR China
[b] Integrated Composites Laboratory (ICL), Department of Chemical & Biomolecular Engineering, University of Tennessee, Knoxville, TN 37996, USA
[c] Ministry-of-Education Key Laboratory of Fluid Mechanics, Beihang University, Beijing 100191, PR China

ARTICLE INFO

ABSTRACT

Based on the phenomena of the embedding dusts on the surface of fresh paint film, industrialized hydrophobic R974 nanoparticles were used as "dust", and epoxy resin was used as "paint" to prepare the superhydrophobic film with high bonding strength. The superhydrophobic film was fabricated by spraying the R974-ethanol suspension onto the dip-coated epoxy resin film on glass slide. Because the epoxy resin acted as bonding layer between the R974 nanoparticles film and the glass slide, a combination of high bonding strength and superhydrophobicity was achieved. The superhydrophobic surface was characterized by water contact angle measurements and scanning electron microscopy (SEM). The water contact angle of the R974 coating could reach 154.7°, and the significant differences in the surface morphology of superhydrophobic coating were presented with different R974 concentrations. A flat, fractal-like texture was observed for coatings sprayed with low R974 concentration, and a rough, porous surface for coatings sprayed with high R974 concentration. The adhesion between the R974 coating and epoxy resin was evaluated by the adhesive-tape test. The interaction between fractal-like aggregated R974 with epoxy resin was large enough because of the surface-to-surface contact mode, and the interaction between microparticles of aggregated R974 with the epoxy resin was weak because of the point-to-surface contact mode. By comparing the skin friction drag on normal surface with the prepared superhydrophobic surface, the superhydrophobic coatings achieved a 12% drag reduction in water.

© 2016 Published by Elsevier B.V.

1. Introduction

The surface with water contact angle over 150° and sliding angle lower than 10° is generally classified as superhydrophobic surface [1]. The superhydrophobic surface has drawn considerable attentions for both fundamental research and practical applications in the past 15 years, such as in self-cleaning [2–6], anticorrosion [7–9], anti-ice [10,11], drag-reduction [12–15], and so forth. It is widely known that a micro-/nano-scale hierarchical surface structure and a low surface energy are two key factors for superhydrophobic surface. In recent research, nanoparticle is a promising material to prepare superhydrophobic coatings, because the nanoparticle aggregates usually have multi-scale roughness including the nano-scale of primary nanoparticles and the micro-scale roughness of nanoparticle aggregates [16]. The general process of fabricating superhydrophobic surface using nanoparticles involves two steps: the hierarchical rough surface is created with nanoparticles and then modified with low surface energy materials

[17–22]. In order to simplify the general two-step process, hydrophobic nanoparticles were used directly to produce the superhydrophobic surface in one step without post-treatment, because of the assembly of hydrophobic nanoparticles could provide both surface hydrophobicity and surface roughness. More hydrophobic nanoparticles were used for superhydrophobic surfaces fabrication, such as silane coupling agent modified silica nanoparticles [23–26], carbon nanotubes [27], stearic acid modified ZnO [28], pigment nanoparticles [29], and so on.

The resistance to mechanical tear and wear of the superhydrophobic surface is an important factor to determine its practical applications. In order to enhance the adhesion between the superhydrophobic coating and substrate, the bonding layer [30,31] and nanoparticle/polymer blends [16,32–35] have recently been applied as a route. Cholewinski and co-workers [30] reported a facile dip-coating process that embedded micron-scale polydimethylsiloxane (PDMS)-functionalized silica particles with nano-scale roughness into an epoxy layer, the use of epoxy pre-layer enhanced the bonding strength of the embedded nanoparticles. Zhang and co-workers [34] have reported superhydrophobic coating fabrication by spraying an alcohol solution consisting of R974 hydrophobic silica nanoparticles and methyl silicate precursor, the methyl silicate precursor played as a binder between nanoparticles and substrate. Ge and co-workers [35] reported that the superhydrophobic

---

coating could be prepared by spraying fluoroalkyl silane nano-SiO$_2$ and methylsiloxane isopropanol suspension on the glass, and methylsiloxane was introduced to enhance the wetting and adhesion of the hydrophobic SiO$_2$ nanoparticles on the hydrophilic glass slide after curing. In the case of nanoparticle/polymer blends, the polymer concentration is very important to fabricate high adhesion superhydrophobic coating. The concentration below the optimal value (a balanced consideration of the adhesion and the hydrophobicity) resulted in poor adherence of the particles to the substrate, and the concentration over this value resulted in the loss of superhydrophobicity, due to the complete embedment of nanoparticles in the polymer.

Nanoparticles always tend to agglomerate due to their high surface area and surface energy [36]. The interparticle forces within the agglomeration stem from the van der Waals, capillary, and electrostatic forces [37]. In the field of nanocomposites, the agglomeration of nanoparticles in polymer/plastic matrix will decrease the mechanical property of nanocomposites, and an ideal nanocomposite should be free of agglomerates. Although the strong inter-nanoparticle interaction is deleterious for polymer nanocomposites, the severe shear force provided by conventional mixing facilities often fails to break apart the nanoparticle agglomerates [38], the inter nanoparticle interaction would benefit to form strong adhesion between the nanoparticles and the substrate.

In this paper, based on the phenomena of the embedded dusts on the surface of fresh paint film, industrialized hydrophobic R974 nanoparticles were used as "dust", and epoxy resin was used as "paint" to prepare the superhydrophobic film with high bonding strength. The R974 is the industrialized hydrophobic silica nanoparticles, which may simplify the process of superhydrophobic surface fabrication without silane hydrophobic treatment of the nanoparticles. The epoxy resin is a commonly used resin in industry, and can be readily coated on a wide variety of substrates. A simple method for the fabrication of superhydrophobic coating by spraying R974-ethanol suspension onto the epoxy resin pre-coated substrate was studied in this paper. The effect of the R974 concentration on the morphology of the coatings, and the effect of the morphology on the adhesion of R974 coatings on substrate were studied. The superhydrophobic surface was used to reduce the skin friction drag in water and the drag reduction effect was confirmed quantitatively via rotar-water system.

2. Experimental

2.1. Materials

Epoxy resin E51 and curing agent T31 were purchased from Hangzhou Wuhuigang Adhesive Co., Ltd. Aerosil R974 was purchased from Beijing Boyu Gaoke New Material Technology Co., Ltd. Acetone (AR) and ethanol (AR) were purchased from Beijing Beihua Fine Chemicals Co., Ltd. All the agents were used without further purification.

2.2. Preparation of superhydrophobic surface

In experiment, the glass slide was used as the model substrate and was cleaned firstly by ultrasonication (KX-1620, Beijing kexi technology Co., Ltd., China) in ethanol for 30 min and dried at ambient temperature for 2 h prior to use.

The dipping method was used for the fabrication of epoxy pre-coatings. 40 g acetone was mixed mechanically with 40 g E51 at 400 r/min for 30 min, and then 10 g T31 was added into the mixture and stirred for 10 min. In general, the adding of acetone can slow down the curing of epoxy. The epoxy resin is not cured at ambient temperature and this allows the R974 nanoparticles be embedded on the surface of epoxy pre-coatings by spray coating of R974. In experiment, the additive acetone also reduced the viscosity of epoxy resin, and the surface of the epoxy pre-layer became smoother after dip coating. The cleaned glass

slide was then immersed into the prepared epoxy resin solution at the dipping speed of 140 mm/min, after 1 min intervals, the glass slide was withdrawn at the same speed. The sample was then placed vertically and dried 30 min at ambient condition.

The spray-coating method was adopted to prepare the R974 superhydrophobic coating. The R974 nanoparticles were dispersed in ethanol firstly for 10 min by ultrasonication to prevent the aggregation, and only freshly prepared batches of R974 suspension was used. Subsequently, the uniform suspensions were sprayed onto the surface of epoxy pre-coated glass slide. An internal-mix air-atomizing spray nozzle (SU1A, Shanghai shangyang valve factory, China) was used, and the 0.2 MPa compressed air gas was supplied by an external air compressor (WB550-2A50, LIDA machine equipment Co., Ltd., China). The flow capacity of R974 suspension was 5 mL/min controlled by the injection pump (lLSP02-1B, Baoding Longer Precision Pump Co., Ltd., China), and the distance between the spray nozzle and the substrates was 300 mm. During spray-coating, the R974 nanoparticles can be embedded into epoxy resin firstly due to the solubility of epoxy resin monomers in ethanol, forming a transition layer of embedded R974 nanoparticles. The R974 nanoparticles can be deposited on the film of embedded R974 nanoparticles by strong interaction force, and aggregated on the substrates. After spraying for 1 min, the sample was placed in drying oven (DHG 101-00, Shangyu Huyue instrument equipment factory, China) for 2 h at 80 °C to cure the epoxy resin, according to the commercial product specification. The polymerization of epoxy resin then served to form a thin layer of glass-like coating and permanently locked the hydrophobic R974 nanoparticles in place, improving the adhesion.

The concentration of R974 could influence the morphology of the coating and finally affected the hydrophobicity of the surfaces, i.e., the higher concentration of R974 could lead to larger aggregates of R974 nanoparticles. The effect of the R974 concentration (1, 2, 5 and 10 wt%) was studied in this paper.

2.3. Characterization

The wettability of coating surface was evaluated based on the value of water contact angle (CA), which was measured by the drop method using a 4 μL water droplet at room temperature. The water CAs of the samples were measured by OCA 15 Pro goniometer (Dataphysics GMBH, Germany) and averaged over three different fresh spots on each sample.

The morphology of the superhydrophobic coating on the substrates was examined using a Field-emission scanning electron microscope (JSM-6700F, JEOL, Japan) with an accelerating voltage of 5 kV. The samples were sputter-coated with gold before imaging.

Similar to previous work [30,39,40], the tape test was used to character the adhesion between the two-layered hydrophobic coatings and the substrate (glass slides). Briefly, the double-sided adhesive foam tape (1.6 mm thick) was adhered to the coatings firstly, and a 100 g weight was rolled over the tape to ensure consistency. The tape was then peeled back at an angle of approximately 45°, and the peeling procedure was repeated with a new piece of tape each time until a total of seven applications of tape were made. The water contact angles of the coating before and after 1, 3, 5, and 7 applications of tape were measured, and the morphology of the coatings before and after 7 applications of tape were examined to evaluate the durability of coatings.

The drag reduction measurements were implemented using rotary apparatus. A rotary viscometer (NDJ-1, Shanghai Yueping Scientific Instrument Co., Ltd., China) was used to predict the skin friction drag of rotor. In order to evaluate the skin friction drag accurately, a custom-made 200 mm height and 100 mm diameter steel rotor was used at 6 rpm rotation rate (Fig. S1†). The skin friction drag of the hydrophilic polished stainless steel rotor was measured firstly. Subsequently, the rotor was coated with epoxy resin, and 2 wt% R974 solution spray-
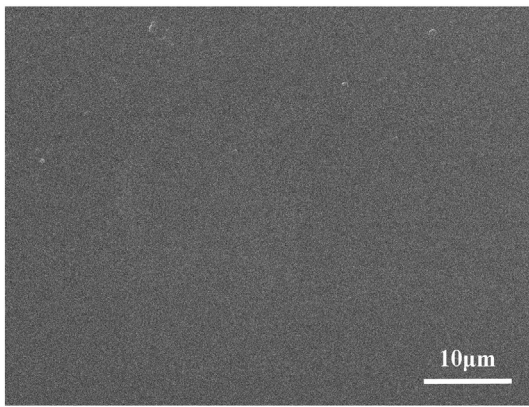
Fig. 1. The morphology of the epoxy resin coated glass slide.
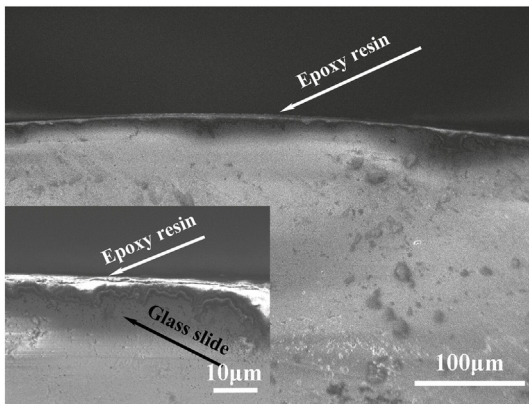

Fig. 2. The morphology of the cross section of epoxy resin coated glass slide.

coated on the surface for 1 min to produce the superhydrophobic rotor, the skin friction drag of superhydrophobic rotor was measured at last. All the operations were performed at room temperature.

3. Results and discussion

The water contact angle of the control sample coated with epoxy only was 68.1°, showing that the surface was also hydrophilic after epoxy resin coating. The morphology of the epoxy resin coated glass slide was smooth at both microscale and nanoscale (Fig. 1). In Fig. 2, the SEM image of the cross section of epoxy resin coated glass slide showed a very smooth and thin layer of epoxy resin, which was around 1 μm in thickness.

Fig. 3 shows the morphology of the R974 films spray-coated with different concentrations of R974. At low concentration (1 wt%, Fig. 3(a)), the surfaces exhibited a smooth morphology with messy gaps at the microscale [41], resulting in a larger fraction of air trapped in the microscale grooves. As the concentration of R974 is increased to 2 wt% (Fig. 3(b)), the width of the messy gaps is larger, and some aggregates of the R974 nanoparticles were deposited on the film. With increasing the concentration of R974 nanoparticles, the epoxy resin precoated substrates are completely covered by a corpuscular layer of sphere-like R974 aggregates (5 wt%, Fig. 3(c)) and a cybotactic layer of irregular and sphere-like R974 aggregates (10 wt%, Fig. 3(d)), which endowed the surface with a highly porous microstructure [21, 33]. Additionally, from the higher magnification images (Fig. S2†), the nanoscale structures was observed more clearly. As shown in the high magnification image, a compact distribution of R974 nanoparticles at the nanoscale shows that the presence of nano-scale roughness being superimposed on the micro-scale morphology of the R974 films. Significant differences in the surface morphology were noted that a flat, fractal-like texture for coatings sprayed with low concentration as compared to a rough, porous surface for coatings sprayed with high concentration. The results indicated that the hierarchical surface structure was present in all R974 films, and the necessary rough structures for superhydrophobicity have been garnered by the spray coating method.

The relationships between morphology and concentration of R974 can be explained by considering the solvent evaporation during spray atomization and R974 nanoparticles deposition. After atomization, the R974-ethanol suspension traveled through air from the nozzle to the substrate in the form of droplets. At lower concentration (1 and 2 wt%), the droplets contained more solvent and only part of solvent
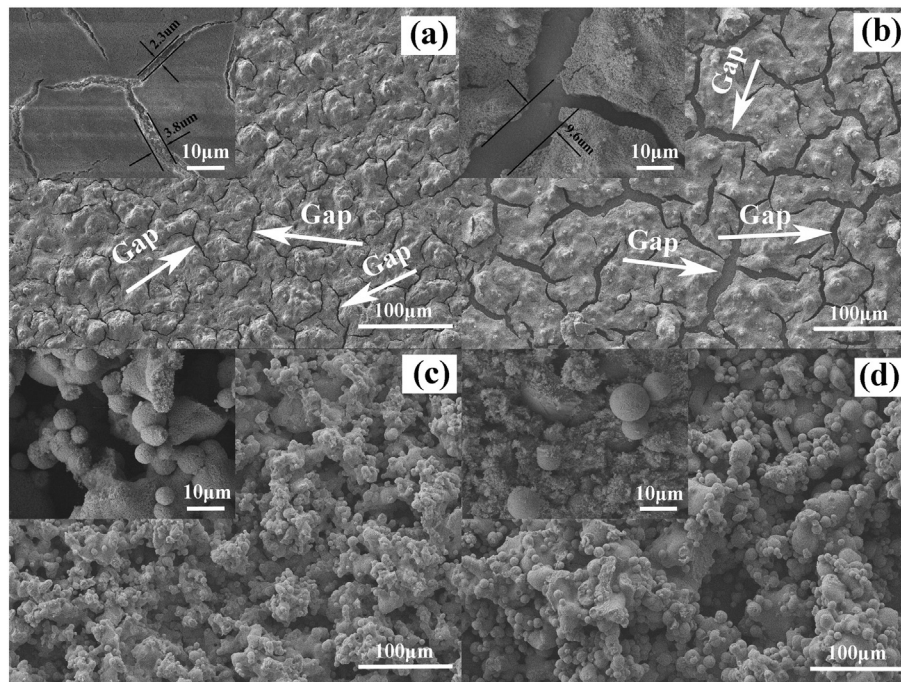

Fig. 3. The morphology of R974 coatings at a R974 concentration of (a) 1, (b) 2, (c) 5, and (d) 10 wt%.
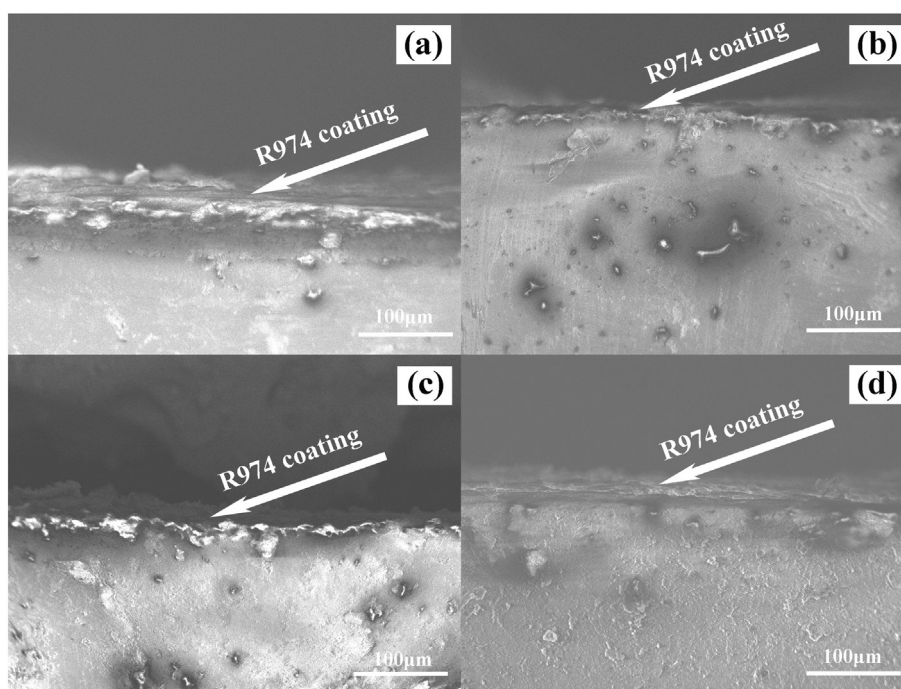
Fig. 4. The morphology of the cross section of R974 coatings at a R974 concentration of (a) 1, (b) 2, (c) 5, and (d) 10 wt%.

was evaporated before the droplets impact on the substrate surface. A "wet" coating with a thin liquid film was formed on the surface of substrate during spray coating, and a relatively smooth film with messy gaps was formed after drying (Fig. 3 (a) & (b)). In contrast, at higher concentration (5 and 10 wt%), the droplets contained little solvent and majority of solvent was evaporated during the time of flight, leading to large aggregates of R974 nanoparticles and no liquid film was formed, the aggregates of the R974 nanoparticles on the substrate formed a "dry" coating (Fig. 3 (c) & (d)) ultimately.

The SEM images of the cross section of glass slide spray-coated by different R974 concentrations with epoxy resin pre-layer are shown in Fig. 4. Compared with the images of the cross section of epoxy resin coated glass slide, a thin and smooth epoxy resin layer was seen clearly in Fig. 2 without R974 layer. However, a thin and rough R974 coating was observed on the surface of glass slide, and the R974 layer and epoxy resin layer were not distinguished clearly in Fig. 4. In the high magnification images (Fig. S3†), more R974 residues were observed to connect with the R974 layer, and covered on the surface of cross section, which made it difficult to distinguish the R974 layer and epoxy resin layer. From another angle, the aggregate force between R974 nanoparticles was strong enough to make the R974 residues connected with the R974 coating.

To identify the wettability of R974 coating, both qualitative and quantitative tests were carried out. The R974 coatings were extremely slippery relative to water, and the water droplets in the form of beads quickly rolled off the surface even at a small inclination (as shown in Supplementary Movie 1), indicating that the observed superhydrophobicity was in Cassie-Baxter state (in which air trapped in the microscale grooves) [42]. Fig. 5 shows the relationship between the concentration values of R974 and the water contact angles on the superhydrophobic coating. From Fig. 5, it can be seen that the water contact angle is 148.8° when the R974 concentration was 1 wt%, close to 150°. The water contact angle was 154.7° as the R974 concentration was increased to 2 wt%, indicating a superhydrophobic surface. This difference can be analyzed by the Cassie–Baxter model [43], based on which the R974 coating is thought of comprising of solid and air pockets, and the hydrophobicity is increased by air trapping. The width of the gaps was about 2 – 4 μm at 1 wt% (Fig. 3(a)) and around 10 μm at 2 wt% (Fig. 3(b)), the roughness was

higher for large-scale dense regions with larger gaps, meaning that more air contacted with water droplet and further generated the superhydrophobicity of surface. The water contact angle was 153.4° and 152.5° with the increase of R974 concentration, causing by the aggregates of R974 at the microscale, and forming a highly porous microstructure. Fig. S4† shows the photographs of water droplets (4 μL) on the epoxy coated glass slide and the 2 wt% R974 spray-coated superhydrophobic glass slide, which was consistent with the results of water contact angles.

Fig. 6 shows the photos of R974 coatings on the glass slides, sprayed by different concentration R974 solutions, before and after the tape test. From the photos, there were two different parts in each glass slide. The bottom half of the glass slides was white, indicating the complete coating of R974 on the surface of pre-coated epoxy film. The upper half of the glass slides was almost transparent, and the R974 nanoparticles were impossible to be coated on the surface of the glass slides without
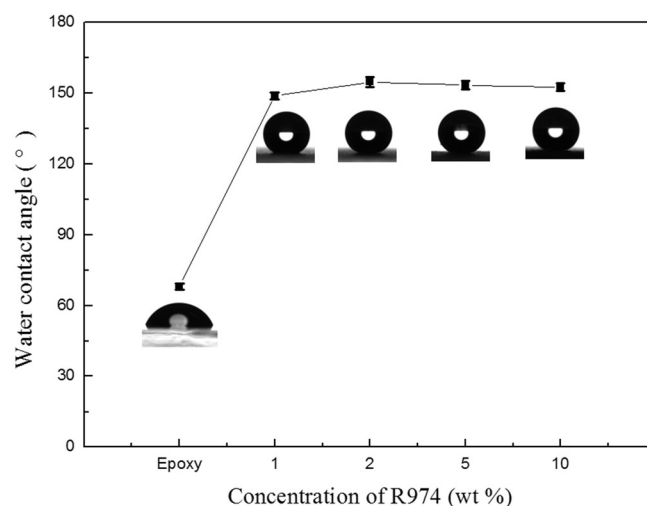

Fig. 5. Wettability of the coating sprayed by the R974 solutions with different concentrations.
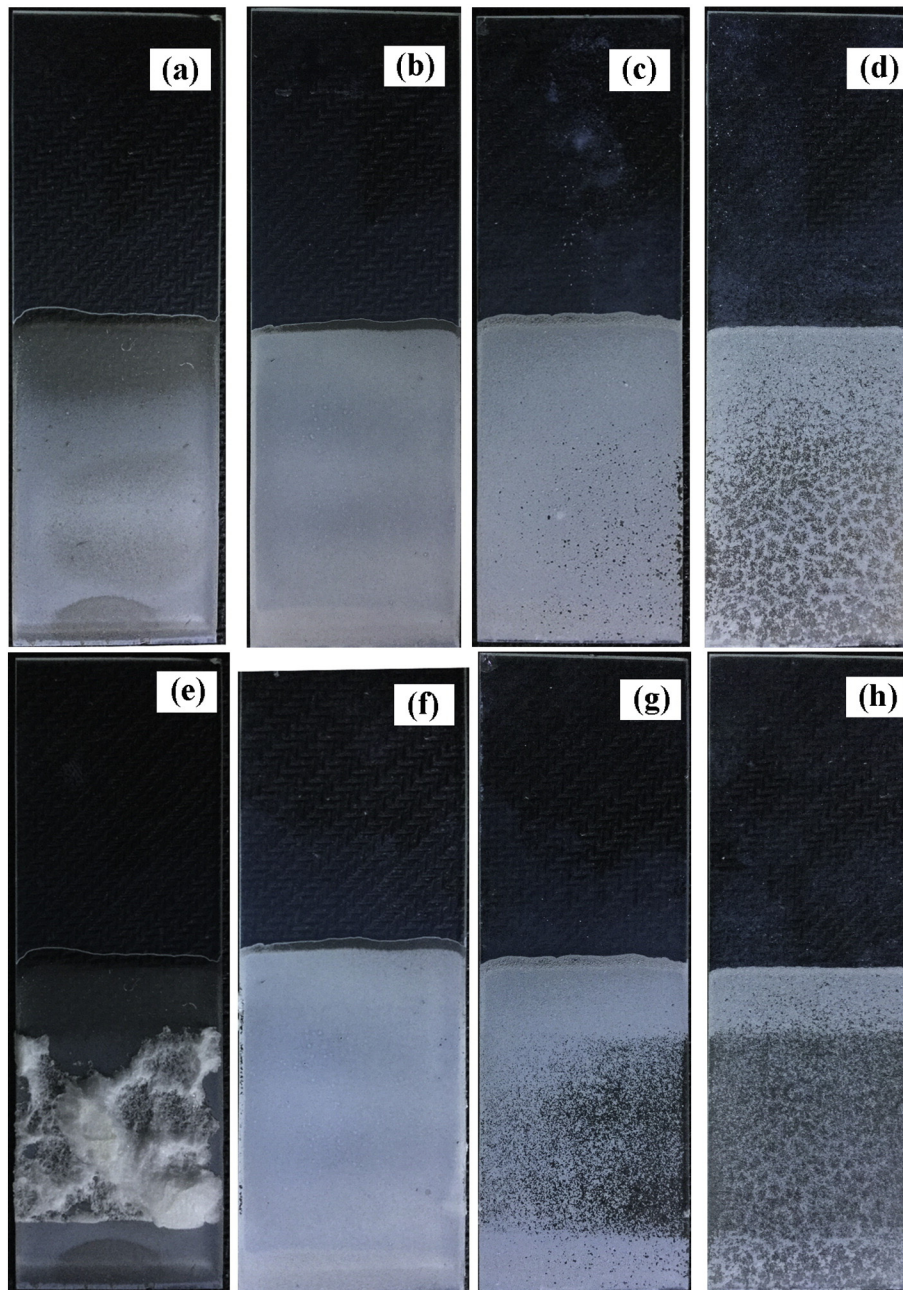
Fig. 6. Photographs of R974 coatings formed by spraying different solution. (a) before and (e) after one-run tape test (1 wt%), (b) before and (f) after 7-run tape test (2 wt%), (c) before and (g) after 7-run tape test (5 wt%), (d) before and (h) after 7-run tape test (10 wt%).

the epoxy resin pre-coatings. From another aspect, this phenomenon indicates that the epoxy resin could enhance the adhesion of the nanoparticles on the substrate as expected [44,45].

Fig. 6 (a) & (e) shows the photographs of the R974 coatings, sprayed with 1 wt% solution, before and after one application of tape test. Major parts of the tape were adhered on the R974 coating after tape test, meaning that the adhesion between the R974 coating and the epoxy resin pre-coatings was larger than the tensile strength of the foam. The photographs of the R974 coatings, sprayed with 2 wt% solution, before and after 7 applications of tape test were shown in Fig. 6 (b)&(f), there were no obvious change before and after the tape test. From Fig. 6 (c), (g), (d) & (h), the R974 coatings, sprayed with 5 wt% and 10 wt% solution, were destroyed after 7 applications of tape test, only parts of the R974 aggregates adhered and remained on the surface of epoxy resin pre-layer after 7-run tape test.

Fig. 7 shows the water contact angles of the coatings, sprayed with different concentration R974 solutions, before and after 1, 3, 5, 7 applications of tape test. The water contact angle was around 153° before and after tape test, as the R974 concentration was 2 wt%. This indicates that the superhydrophobicity was retained after 7 times tape peeling, indicating that the coating is robust. However, when the concentration of R974 was increased to 5 and 10 wt%, the water contact angle of the coating was decreased from 153.4° to 143.7° at 5 wt%, and from 152.5° to 115° at 10 wt% after the tape test. The results indicate that the R974 coatings were destroyed, and the surface was changed from superhydrophobic to hydrophobic after the tape test. According to the above experimental results, it can be concluded that the most durable coating was fabricated when the R974 concentration was 2 wt%.

Fig. 8 shows the morphology of the R974 films before and after 7 applications of tape test at different concentrations of R974. From Fig. 8 (a)
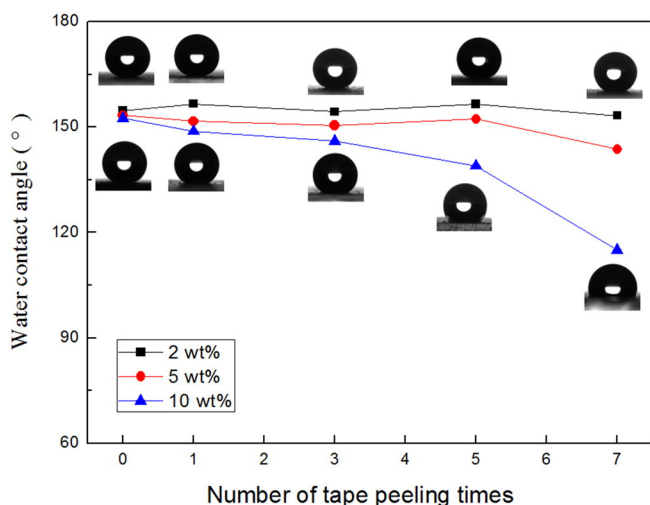
Fig. 7. Water contact angles of the coatings with different R974 concentration before and after 1, 3, 5, 7 applications of tape test.

& (b), it can be seen that only the microparticles of aggregated R974 on the protrusions adhered to the R974 layer are removed after the tape peeling, the flat fractal-like aggregated R974 were left behind, meaning that the interaction between fractal-like aggregated R974 with epoxy resin coating was large enough to guarantee a stable surface structure, and the R974 coating was not damaged by the tape peeling. From Fig. 8 (c), (d), (e) & (f), it can be seen that many microparticles of aggregated R974 were removed after the tape peeling, suggesting that the microparticles of aggregated R974 stayed on top of the coating with weak adhesion. The results show that a 'wet' flat coating prepared at low concentration is mechanically stronger than a 'dry' porous coating prepared at high concentration [33].

The simplified schematic of the multilayer film preparation is shown in Fig. 9. Two different models were proposed for the fabrication of multilayer film with low and high concentration of R974 solution. The "wet" coating with a thin liquid film was formed during spray coating at low concentration, and the R974 nanoparticles would rearrange themselves in ethanol by adhesion interactions to form a smooth layer. Because of the solubility of epoxy resin monomers in ethanol, the R974 nanoparticles contacted the epoxy resin, intended to be embedded into the epoxy resin. During the drying procedure, the embedded R974 nanoparticles were locked by the polymerized epoxy resin, and the evaporation of ethanol led to the formation of a self-assembled R974 fractal-like layer. The single R974 nanoparticles provide nanoscale roughness, and the messy gaps provide micro-scale roughness. The necessary rough structures for superhydrophobicity have been garnered. Because of the constant aggregate force of two original R974 nanoparticles, the more contact area means more adhesion force, and the fractal-like
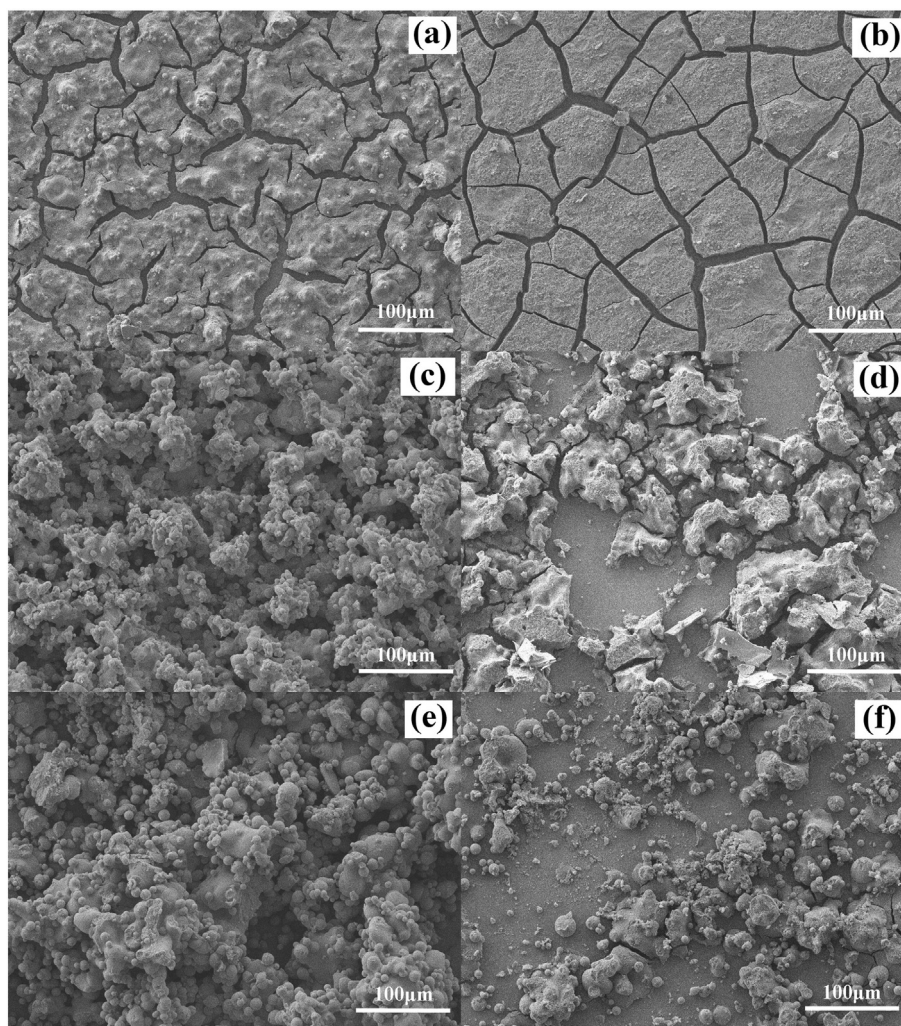

Fig. 8. The morphology of R974 coatings before and after 7-run tape test at different concentrations, 2 wt% before (a) and after (b); 5 wt% before (c) and after (d); 10 wt% before (e) and after (f).
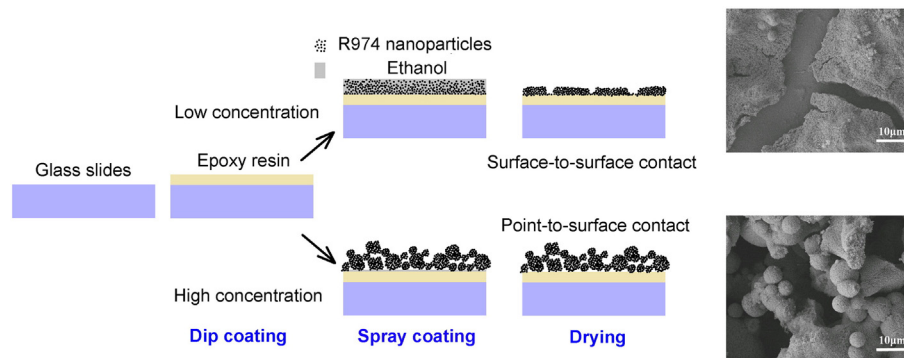
Fig. 9. Simplified schematic of the multilayer film preparation.

aggregated R974 could enhance the bonding strength by the strong surface-to-surface contact mode.

The "dry" coating was formed during the spray coating at high concentration, and the spherical and irregular aggregated R974 nanoparticles would adhere on the surface of epoxy. The spherical aggregated R974 could decrease the bonding strength by the weak point-to-surface contact mode. The two different models for the fabrication of R974 coating can explain that the 'wet' flat coating prepared by low concentration was mechanically stronger than the 'dry' porous coating prepared by high concentration.

Additionally, according to the above results, a different substrate material, the steel piece, was used as a model substrate to demonstrate the process of the superhydrophobic surface fabrication in experiment. The photos of water droplet (4 μL) on epoxy resin coated and R974 spray-coated steel piece are shown in Fig. S5, the water contact angle of epoxy resin coated and R974 spray-coated steel piece was 67.8° and 154.5° respectively, indicating that the surface of epoxy resin coated steel piece changed from hydrophilic to superhydrophobic after 2 wt% R974 spray-coating. The result illustrates that with the epoxy pre-layer, R974 spray-coating method could produce superhydrophobic surface on different substrate materials.

Ignoring the skin friction drag induced by the rotor bottom surface, the torque moment caused by the skin friction drag on the rotor surface could be calculated by Eq. (1):

$$F \times r = k \times \varnothing \tag{1}$$

where F is the skin friction drag on the rotor surface, r is the radius of rotor, k is the coefficient of the balance spring, which is a constant value to the same balance spring, $\varnothing$ is the deflection angle of the balance spring, which can be read in the dial plate. The skin friction drag on rotor surface is proportional to the deflection angle of the balance spring. To experimentally quantify the skin friction drag reduction on different wetting surface, the drag reduction ratio (C_R) was applied and can be calculated from Eq. (2):

$$C_R = \frac{F_n - F_s}{F_n} \times 100\% = \frac{\varnothing_n - \varnothing_s}{\varnothing_n} \times 100\% \tag{2}$$

where F_n and F_s are the skin friction drag on normal surface and superhydrophobic surface, $\varnothing_n$ and $\varnothing_s$ are the pointer deflection of normal surface and superhydrophobic surface.

The water contact angle of polished rotor surface and R974 spray-coated rotor surface was 13.6° and 154.6° (Fig. S6), indicating that the rotor surface was changed from hydrophilic to superhydrophobic after R974 spray-coating. The pointer deflection of the polished stainless steel rotor and the R974 spray-coated rotor was 62.5 and 55, indicating that the R974 coated superhydrophobic rotor achieved a 12% frictional drag reduction when compared with the hydrophilic polished stainless

steel rotor, which is attributed to the shear-reducing air layer entrapped on the superhydrophobic surface [13].

4. Conclusion

The superhydrophobic coatings were fabricated by spraying the R974-ethanol suspension onto the dip-coated epoxy resin film on the glass slide. Because the epoxy resin acted as bonding layer between the R974 nanoparticles film and the glass slide, a combination of high bonding strength and superhydrophobicity were achieved, and the water contact angle of the coating could reach 154.7°. A flat, fractal-like texture was observed for the coatings sprayed with low R974 concentration; and a rough, porous surface for the coatings sprayed with high R974 concentration. The strong interaction between the fractal-like aggregated R974 with epoxy resin in the coating with low R974 concentration was due to the strong surface-to-surface contact mode; while the weak interaction between microparticles of aggregated R974 with the epoxy resin was caused by the weak point-to-surface contact mode. The superhydrophobic coatings achieved a 12% frictional drag reduction in water. This study provides an easy and simple method to obtain superhydrophobic coatings with high bonding strength.

Supplementary data to this article can be found online at http://dx.doi.org/10.1016/j.surfcoat.2016.09.009.

References

[1] S. Wang, L. Jiang, Definition of superhydrophobic states, Adv. Mater. 19 (2007) 3423–3424.
[2] S.S. Latthe, P. Sudhagar, C. Ravidhas, A.J. Christy, D.D. Kirubakaran, R. Venkatesh, A. Devadoss, C. Terashima, K. Nakata, A. Fujishima, Self-cleaning and superhydrophobic CuO coating by jet-nebulizer spray pyrolysis technique, CrystEngComm 17 (2015) 2624–2628.
[3] S.S. Latthe, C. Terashima, K. Nakata, M. Sakai, A. Fujishima, Development of sol–gel processed semi-transparent and self-cleaning superhydrophobic coatings, J. Mater. Chem. A 2 (2014) 5548–5553.
[4] X. Zhang, Y. Guo, Z. Zhang, P. Zhang, Self-cleaning superhydrophobic surface based on titanium dioxide nanowires combined with polydimethylsiloxane, Appl. Surf. Sci. 284 (2013) 319–323.
[5] D. Ge, L. Yang, Y. Zhang, Y. Rahmawan, S. Yang, Transparent and superamphiphobic surfaces from one-step spray coating of stringed silica nanoparticle/Sol solutions, Part. Part. Syst. Charact. 31 (2014) 763–770.
[6] J. Liu, J. Huang, E.K. Wujcik, B. Qiu, D. Rutman, X. Zhang, E. Salazard, S. Wei, Z. Guo, Hydrophobic electrospun polyimide Nanofibers for self-cleaning materials, Macromol. Mater. Eng. 300 (2015) 358–368.
[7] J. Li, R. Wu, Z. Jing, L. Yan, F. Zha, Z. Lei, One-step spray-coating process for the fabrication of colorful superhydrophobic coatings with excellent corrosion resistance, Langmuir 31 (2015) 10702–10707.

[8] F. Su, K. Yao, Facile fabrication of superhydrophobic surface with excellent mechanical abrasion and corrosion resistance on copper substrate by a novel method, ACS Appl. Mater. Interfaces 6 (2014) 8762–8770.

[9] Y. Hu, S. Huang, S. Liu, W. Pan, A corrosion-resistance superhydrophobic TiO$_2$ film, Appl. Surf. Sci. 258 (2012) 7460–7464.

[10] P. Kim, T.-S. Wong, J. Alvarenga, M.J. Kreder, W.E. Adorno-Martinez, J. Aizenberg, Liquid-infused nanostructured surfaces with extreme *anti*-ice and anti-frost performance, ACS Nano 6 (2012) 6569–6577.

[11] L.B. Boinovich, A.M. Emelyanenko, V.K. Ivanov, A.S. Pashinin, Durable icephobic coating for stainless steel, ACS Appl. Mater. Interfaces 5 (2013) 2549–2554.

[12] Y. Wang, X. Liu, H. Zhang, Z. Zhou, Superhydrophobic surfaces created by a one-step solution-immersion process and their drag-reduction effect on water, RSC Adv. 5 (2015) 18909–18914.

[13] E. Aljallis, M.A. Sarshar, R. Datla, V. Sikka, A. Jones, C.-H. Choi, Experimental study of skin friction drag reduction on superhydrophobic flat plates in high Reynolds number boundary layer flow, Phys. Fluids 25 (2013) 025103.

[14] H. Dong, M. Cheng, Y. Zhang, H. Wei, F. Shi, Extraordinary drag-reducing effect of a superhydrophobic coating on a macroscopic model ship at high speed, J. Mater. Chem. A 1 (2013) 5886–5891.

[15] S. Srinivasan, W. Choi, K.-C. Park, S.S. Chhatre, R.E. Cohen, G.H. McKinley, Drag reduction for viscous laminar flow on spray-coated non-wetting surfaces, Soft Matter 9 (2013) 5691–5702.

[16] Z. He, M. Ma, X. Xu, J. Wang, F. Chen, H. Deng, K. Wang, Q. Zhang, Q. Fu, Fabrication of superhydrophobic coating via a facile and versatile method based on nanoparticle aggregates, Appl. Surf. Sci. 258 (2012) 2544–2550.

[17] Q. Shang, Y. Zhou, G. Xiao, A simple method for the fabrication of silica-based superhydrophobic surfaces, J. Coat. Technol. Res. 11 (2014) 509–515.

[18] J.-Y. Kim, E.-K. Kim, S.S. Kim, Micro-nano hierarchical superhydrophobic electrospray-synthesized silica layers, J. Colloid Interface Sci. 392 (2013) 376–381.

[19] E.-K. Kim, C.-S. Lee, S.S. Kim, Superhydrophobicity of electrospray-synthesized fluorinated silica layers, J. Colloid Interface Sci. 368 (2012) 599–602.

[20] L. Xu, J. He, Fabrication of highly transparent superhydrophobic coatings from hollow silica nanoparticles, Langmuir 28 (2012) 7512–7518.

[21] J. Bravo, L. Zhai, Z. Wu, R.E. Cohen, M.F. Rubner, Transparent superhydrophobic films based on silica nanoparticles, Langmuir 23 (2007) 7293–7298.

[22] F. Li, M. Du, Q. Zheng, Transparent and durable SiO$_2$-containing superhydrophobic coatings on glass, J. Appl. Polym. Sci. 132 (2015).

[23] H. Ogihara, J. Xie, T. Saji, Controlling surface energy of glass substrates to prepare superhydrophobic and transparent films from silica nanoparticle suspensions, J. Colloid Interface Sci. 437 (2015) 24–27.

[24] H. Ogihara, J. Xie, T. Saji, Factors determining wettability of superhydrophobic paper prepared by spraying nanoparticle suspensions, Colloids Surf. A Physicochem. Eng. Asp. 434 (2013) 35–41.

[25] H. Ogihara, J. Xie, J. Okagaki, T. Saji, Simple method for preparing superhydrophobic paper: spray-deposited hydrophobic silica nanoparticle coatings exhibit high water-repellency and transparency, Langmuir 28 (2012) 4605–4608.

[26] J. Li, H. Wan, Y. Ye, H. Zhou, J. Chen, One-step process to fabrication of transparent superhydrophobic SiO$_2$ paper, Appl. Surf. Sci. 261 (2012) 470–472.

[27] H. Ogihara, J. Xie, T. Saji, Spraying carbon nanotube dispersions to prepare superhydrophobic films, J. Mater. Sci. 49 (2014) 3183–3188.

[28] J. Li, Z. Jing, Y. Yang, F. Zha, L. Yan, Z. Lei, Reversible low adhesive to high adhesive superhydrophobicity transition on ZnO nanoparticle surfaces, Appl. Surf. Sci. 289 (2014) 1–5.

[29] H. Ogihara, J. Okagaki, T. Saji, Facile fabrication of colored superhydrophobic coatings by spraying a pigment nanoparticle suspension, Langmuir 27 (2011) 9069–9072.

[30] A. Cholewinski, J. Trinidad, B. McDonald, B. Zhao, Bio-inspired polydimethylsiloxane-functionalized silica particles-epoxy bilayer as a robust superhydrophobic surface coating, Surf. Coat. Technol. 254 (2014) 230–237.

[31] C. Su, J. Li, H. Geng, Q. Wang, Q. Chen, Fabrication of an optically transparent superhydrophobic surface via embedding nano-silica, Appl. Surf. Sci. 253 (2006) 2633–2636.

[32] R. Karmouch, G.G. Ross, Superhydrophobic wind turbine blade surfaces obtained by a simple deposition of silica nanoparticles embedded in epoxy, Appl. Surf. Sci. 257 (2010) 665–669.

[33] Y.H. Yeong, A. Davis, A. Steele, E. Loth, I.S. Bayer, Spray deposition effects on superhydrophobicity and durability of nanocoatings, Surf. Innov. 2 (2014) 70–78.

[34] Y. Zhang, D. Ge, S. Yang, Spray-coating of superhydrophobic aluminum alloys with enhanced mechanical robustness, J. Colloid Interface Sci. 423 (2014) 101–107.

[35] D. Ge, L. Yang, G. Wu, S. Yang, Spray coating of superhydrophobic and angle-independent coloured films, Chem. Commun. 50 (2014) 2469–2472.

[36] Y. Raichman, M. Kazakevich, E. Rabkin, Y. Tsur, Inter-nanoparticle bonds in agglomerates studied by nanoindentation, Adv. Mater. 18 (2006) 2028–2030.

[37] P. Begat, D.A. Morton, J.N. Staniforth, R. Price, The cohesive-adhesive balances in dry powder inhaler formulations I: direct quantification by atomic force microscopy, Pharm. Res. 21 (2004) 1591–1597.

[38] M. Rong, M. Zhang, W. Ruan, Surface modification of nanoscale fillers for improving properties of polymer nanocomposites: a review, Mater. Sci. Technol. 22 (2006) 787–796.

[39] A. Steele, I. Bayer, E. Loth, Adhesion strength and superhydrophobicity of polyurethane/organoclay nanocomposite coatings, J. Appl. Polym. Sci. 125 (2012) E445–E452.

[40] H. Hou, Y. Chen, Preparation of super-hydrophobic silica films with visible light transmission using phase separation, J. Sol-Gel Sci. Technol. 43 (2007) 53–57.

[41] I.S. Bayer, A. Brown, A. Steele, E. Loth, Transforming anaerobic adhesives into highly durable and abrasion resistant superhydrophobic organoclay nanocomposite films: a new hybrid spray adhesive for tough superhydrophobicity, Appl. Phys. Express 2 (2009) 125003.

[42] B.J. Sparks, E.F. Hoff, L. Xiong, J.T. Goetz, D.L. Patton, Superhydrophobic hybrid inorganic–organic thiol-ene surfaces fabricated via spray-deposition and photopolymerization, ACS Appl. Mater. Interfaces 5 (2013) 1811–1817.

[43] B. Wang, Z. Mao, X. Meng, W. Tong, C. Gao, Fabrication of cellular polycaprolactone films for cell culture, Colloids Surf. B 76 (2010) 38–43.

[44] H. Gu, C. Mao, J. Gu, J. Guo, X. Yan, J. Huang, Q. Zhang, Z. Guo, An overview of multifunctional epoxy nanocomposites, J. Mater. Chem. C 4 (2016) 5890–5906.

[45] H. Gu, J. Guo, H. Wei, S. Guo, J. Liu, Y. Huang, M.A. Khan, X. Wang, D.P. Young, S. Wei, Z. Guo, Strengthened magnetoresistive epoxy nanocomposite papers derived from synergistic Nanomagnetite-carbon nanofiber nanohybrids, Adv. Mater. 27 (2015) 6277–6282.